

Noise-induced topological transformations of vortex solitons in optical fibers filled with a cold atomic gas

A.V. Prokhorov,^{1,*} M.G. Gladush,² M.Yu. Gubin,¹ A.Yu. Leksin,¹ and S.M. Arakelian¹

¹*Department of Physics and Applied Mathematics,*

Stoletovs Vladimir State University, Gorky str. 87, Vladimir, 600000, Russia

²*Institute for Spectroscopy of the Russian Academy of Sciences,*

Fizicheskaya Str. 5, Troitsk, Moscow, 142190, Russia

(Dated: October 29, 2018)

We consider the influence of optical and temperature-dependent atomic fluctuations on the formation and propagation of optical vortex solitons in dense media realized as hollow-core optical fibers filled with a cold atomic gas in presence of optical pumping. We show different perturbation-induced scenarios of complete destruction and smooth transformation of the topological characteristics of localized optical patterns in hollow-core fiber. The maximum levels of optical and atomic fluctuations at which the soliton regime can be maintained has been determined. The estimates for these levels show that it is possible to observe the optical vortex solitons in the core-filling gas of the fiber for temperatures smaller than the critical temperature of Bose-Einstein condensate.

I. INTRODUCTION

The investigation of the formation and propagation of the localized spatial optical structures in different media [1] is of high interest to modern atomic physics. The importance of this topic is associated with a wide range of applications, such as data transmission and processing [2]. Among optical localized patterns, the greatest interest represents the special class of optical topological structures known as optical vortices [3]. The dark center of those structures could be registered reliably in experiments even in the case of a strong diffraction broadening of the optical beams [4]. It is relatively easy to realize such structures in laser cavities [5] or spatially inhomogeneous media [6]. However, maintaining of the stability conditions for such structures when they propagate in the real media is challenging. The soliton modes of optical vortices have so far been observed quite rarely even within short distances [7]. At the same time, the distances for commercial telecommunications have not been worked out at all. This can be explained by the fact that a full scale solution to the problem of developing such information channels requires a correct determination of the stability regions [8] under the experimental conditions, as well as the stability tests with perturbations for the propagating localized optical structures.

The formation of such stable optical structures occurs near the lasing threshold [2] where the nonlinear effects are very strong. Therefore the identification and analysis of the ranges of parameters at which the optical solitons are stable requires a strict accounting of the higher-order nonlinearities and nonlinear absorption effects in the system [2, 9]. In order to experimentally realize an optical control over the nonlinear and dissipative parameters, it is the most beneficial to use the atomic Λ -scheme of interaction between the localized structure of the probe and

the pump fields. The observations of the strong nonlinear effects in such a scheme can be associated with the realization of the Raman regime [9, 10] when the detunings of the electromagnetic fields from the atomic transitions are much higher than the corresponding decay rates (with the account of the optical depth of the medium, see [11]).

Among promising media for observation and control of solitons, we can mark out recently created hollow-core optical fibres filled with a cold atomic gas [12]. First, it would allow us to observe the coherent Raman scattering and to study the competition between the nonlinear, diffraction and dissipative effects for the probe pulse over short distances [13, 14]. Second, the use of cold atoms opens new possibilities of precision and efficient control over the optical properties of the system. Indeed, in a cold medium we can neglect the effects of the spectral line broadening and splitting typical for hot atoms and solids.

It is a well known fact that the quality of transmission and the processing of information in the optical data channel [15] is strongly dependent on the efficiency of the nonlinear transformations, which increases significantly with the increase of the density of the resonant atoms in the medium. However, for the media with a large density of optically active particles, it is necessary to take into account the effective or the local value of the field acting on them [16–20]. The atom-field interaction in this case becomes more complicated. It is known in the literature as the consequence of the near dipole-dipole interactions (NDD). This may significantly modify the picture of the phenomenon as the conventional Rabi frequency for an atomic transition is comparable to the corresponding NDD correction term. The estimations for ensembles of the resonant particles show that the NDD or the local field effects may be very significant starting from the density $\rho = 10^{15} \text{ cm}^{-3}$. Due to this fact, a special attention should be paid to the problem of obtaining stable dynamics of spatial solitons and optical vortices in particular [3] in dense media with the additional accounting

* avprokhorov@vlsu.ru

of perturbations in the medium and the field.

The influence of the noise effects on the soliton solutions of the nonlinear Schrödinger equation (NLS) has been well studied in the literature, and a violation of the dynamic equilibrium in such a system is typically observed for the values of the noise intensity comparable to the average parameters of the problem [21]. A particularly strong presence of the noise in this problem manifests itself near the zero dispersion point where the short-term noise-induced changes of the dispersion sign would quickly destroy the soliton. The soliton condition in the such system can only be restored by an original pinning method [22]. Analysis of the fluctuations influence on the dissipative solitons is usually performed artificially by introducing a noise source to the Ginzburg-Landau equation (GLE) [23, 24]. However, this approach does not reveal the nature of the noise, and it is therefore not possible to assess the contribution of various physical processes into the development of instabilities in the system. This is especially true in the case of the optical solitons in gaseous media, where the density fluctuations at small scales can be comparable with the average values of density [25, 26]. Even transition to the Bose-Einstein condensate (BEC) can not solve the problem completely because in such a system there are intricate dependencies of density fluctuations on the trapping geometry and the type of interaction between the particles [27, 28].

In this paper, we consider the problem of obtaining a stable spatial dynamics of optical vortices [3] in the dense media of gas-filled hollow-core optical fibers in the presence of an optical pumping. The problem is similar to the observation of temporal self-induced transparency solitons in microstructured materials under the conditions of the influence of the local field effects [18]. We also study the influence of random and/or periodic perturbations of the system's parameters on the process of stabilization and shape evolution during propagation of the vortex solitons.

This paper is structured as follows. In Section II we present our formalism which contains the material equations derived from the Bogolyubov-Born-Green-Kirkwood-Yvon (BBGKY) hierarchy for reduced density matrices and correlation operators for a three-level atomic medium containing the local field effects in the interaction of individual impurity particles with electromagnetic fields. We study the temporal dynamics of the density matrix for the case of the Λ -configuration Raman interaction mode using optical vortices. The requirements for the atomic medium and the optical fields which allow a significant simplification of the problem are formulated. We as well analyze the spatial effects that arise in a self-consistent problem of the nonlinear scattering of the probe field in a dense medium of three-level atoms. We show the possibility to reduce the problem to the fifth-order nonlinear Ginzburg-Landau equation. In Section III we use the variational methods and direct numerical simulation to determine the stability regions

of spatial vortex solitons. In Section IV we describe the stability stress testing of optical vortices under perturbations of system's parameters. The main results and recommendations for the use of BEC-filled hollow fibers as information channels with dissipative vortex solitons is presented in Conclusion.

II. GENERALIZED DENSITY MATRIX EQUATIONS FOR Λ -TYPE ATOM-FIELD INTERACTION IN A DENSE MEDIUM

In this paper, we assume that a probe light beam of a given shape \mathbf{E}_p with the center frequency ω_p propagates along the z axis of a hollow-core optical fiber filled with a gas of cold atoms at a temperature T near the critical temperature [29] of the phase transition:

$$T_{cr} = \frac{\hbar\omega_0}{k_B} \left(\frac{N}{\zeta(3)} \right)^{1/3},$$

where \hbar is the Planck constant, k_B is the Boltzmann constant, N is the total number of particles, ω_0 is the trapping frequency, and $\zeta(3)$ is the zeta function of Riemann. It propagates in the direction opposite to cw pump radiation \mathbf{E}_c as illustrated in Fig. 1a. In the Raman limit for the Λ -scheme of interaction the probe field detuning Δ_b should be substantially greater than the relaxation rate Γ_{ab} (Γ_{ac}) from the excited state $|a\rangle$ (see Fig. 1b). This regime can be used for the formation of spatial optical solitons in the field of the probe radiation \mathbf{E}_p . As applied to this problem, the optical depth of the medium d_0 is determined through the characteristic linear dimension a_0 of topological structures formed in the XY plane as $d_0 = g^2 N a_0 / (c \Gamma_{ac})$ (compare with [10]). Here $g = \mu_{ba} \sqrt{\omega / 2 \hbar \varepsilon_0 V}$ is the atom-field coupling constant, $\varepsilon = A_p \sqrt{2 \varepsilon_0 V / \hbar \omega}$, A_p is slowly varying amplitude of the probe field, V is the quantization volume, $N = \rho V_0$ is the number of atoms in the interaction zone of volume V_0 for atomic density ρ , c is the speed of light in vacuum, ε_0 is the vacuum permittivity. The frequency separation between levels $|b\rangle$ and $|c\rangle$ is $\delta = 6.834 \times 10^9 \text{ s}^{-1}$, the dipole transition matrix element for $|b\rangle \rightarrow |a\rangle$ is $\mu_{ba} = 3.58 \times 10^{-29} \text{ C}\cdot\text{m}$.

Taking into account the large dipole moments of the desired transitions of ^{87}Rb atoms, and the value of their density inside the hollow core fiber, one can conclude that the value of the NDD interactions $\chi_{ba} = \rho |\mu_{ba}|^2 / (3 \hbar \varepsilon_0)$ which determines the effective Rabi frequency $\Omega_{eff} = \Omega_{ba} + \chi_{ba} \sigma_{ba}$ [18] can be close to the value of the Rabi frequency of the probe field. Here σ_{ba} is the corresponding of the density matrix element. Thus, the nonlinear optical effects arising in such a system will be determined, on one hand, by the pump field parameters, and on the other hand, by the number density of the atoms hosted by the hollow fiber.

This system is described by the following set of equations for the density matrix elements:

$$\begin{aligned}
\dot{\sigma}_{ba} &= i(\Delta_b - \chi_{ba}(\sigma_{bb} - \sigma_{aa}))\sigma_{ba} - ig\varepsilon(\sigma_{bb} - \sigma_{aa}) - i(\Omega + \chi_{ca}\sigma_{ca})\sigma_{bc} - \frac{1}{2}(\Gamma_{ab} + \Gamma_{ac})\sigma_{ba}, \\
\dot{\sigma}_{ca} &= i(\Delta_c - \chi_{ca}(\sigma_{cc} - \sigma_{aa}))\sigma_{ca} - i\Omega(\sigma_{cc} - \sigma_{aa}) - i(g\varepsilon + \chi_{ba}\sigma_{ba})\sigma_{cb} - \frac{1}{2}(\Gamma_{ab} + \Gamma_{ac})\sigma_{ca}, \\
\dot{\sigma}_{bc} &= i(\Delta_b - \Delta_c)\sigma_{bc} + ig\varepsilon\sigma_{ac} - i\Omega^*\sigma_{ba} + i\chi_{ba}\sigma_{ba}\sigma_{ac} - i\chi_{ac}\sigma_{ac}\sigma_{ba}, \\
\dot{\sigma}_{aa} &= ig\varepsilon^*\sigma_{ba} + i\Omega^*\sigma_{ca} - ig\varepsilon\sigma_{ab} - i\Omega^*\sigma_{ac} - (\Gamma_{ab} + \Gamma_{ac})\sigma_{aa}, \\
\dot{\sigma}_{bb} &= ig\varepsilon\sigma_{ab} - ig\varepsilon^*\sigma_{ba} + \Gamma_{ab}\sigma_{aa}, \\
\dot{\sigma}_{cc} &= i\Omega\sigma_{ac} - i\Omega^*\sigma_{ca} + \Gamma_{ac}\sigma_{aa},
\end{aligned} \tag{1}$$

where $\Omega \equiv \Omega_{ca}$ and $g\varepsilon \equiv \Omega_{ba}$ are the Rabi frequencies for the pump field and the probe beam, respectively, and Δ_b and Δ_c are the corresponding detunings.

Let us to consider applicability of the approximations for Eqs. (1) under the condition of the specific requirements for our problem. One of these requirements is the presence of a significant polarization of the medium produced by the contiguous transitions $|a\rangle \rightarrow |b\rangle$ and $|a\rangle \rightarrow |c\rangle$. It is necessary to provide nonlinear control over the probe vortices via the pump wave. The key point here is to choose the right balance between the Rabi frequency of the pump field, its detuning from the resonance and the decay rate of the excited state.

In general, the propagation equation for a probe field in a resonant medium is

$$\left(\frac{\partial}{\partial t} + c \frac{\partial}{\partial z} - ic \frac{D}{2} \nabla_{\perp}^2 \right) \varepsilon = -igN\sigma_{ba}, \tag{2}$$

where $\nabla_{\perp}^2 = \partial^2/\partial x^2 + \partial^2/\partial y^2$, and $D = \lambda/\pi$ is the diffraction parameter in the plane transverse to the axis z .

In order to solve the self-consistent problem of Eqs. (1)-(2) we assume, firstly, that all atoms are initially at the

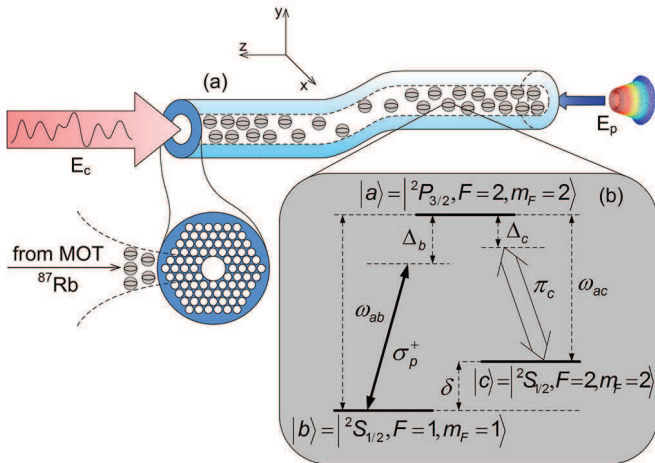


Figure 1. (a) Model diagram of a hollow-core optical fiber filled with an atomic gas (b) Λ -type interaction configuration applied for ^{87}Rb atoms, energy level splitting between $|c\rangle$ and $|b\rangle$ is $\delta = 6.834 \times 10^9 \text{ s}^{-1}$, the dipole transition matrix element for $|a\rangle \rightarrow |b\rangle$ at wavelength $\lambda = 780.241 \text{ nm}$ is $\mu_{ab} = 3.58 \times 10^{-29} \text{ C}\cdot\text{m}$.

level b , i.e., $\sigma_{bb} = 1$, $\sigma_{aa} = \sigma_{cc} = 0$, and the population of the excited state remains small throughout the interaction time, i.e., $\sigma_{bb} \cong 1$, $\sigma_{aa(cc)} \cong 0$ (while $\dot{\sigma}_{ii} \cong 0$ where $i = a, b, c$). Secondly, we believe that when $\chi_{ca} = \chi_{ba} = \chi$, the contribution of the local field is comparable to the probe Rabi frequency, but it can be omitted for the pump transition, i.e., $g\varepsilon \geq \sigma_{ba}\chi_{ba}$ and $\Omega \gg \sigma_{ca}\chi_{ca}$. As a result, the final system of equations reduces to the following (simplified) form:

$$\dot{\sigma}_{ba} = -\Gamma_1\sigma_{ba} - ig\varepsilon - i\Omega\sigma_{bc} - i\chi_{ba}\sigma_{ba}, \tag{3a}$$

$$\dot{\sigma}_{ca} = -\Gamma_2\sigma_{ca} - ig\varepsilon\sigma_{cb} - i\chi_{ba}\sigma_{ba}\sigma_{cb}, \tag{3b}$$

$$\dot{\sigma}_{bc} = i\Delta_3\sigma_{bc} + ig\varepsilon\sigma_{ac} - i\Omega^*\sigma_{ba}, \tag{3c}$$

$$\dot{\sigma}_{bb} = ig\varepsilon\sigma_{ab} - ig\varepsilon^*\sigma_{ba}, \tag{3d}$$

where $\Gamma_1 = -i\Delta_b + 1/2(\Gamma_{ab} + \Gamma_{ac})$, $\Gamma_2 = -i\Delta_c + 1/2(\Gamma_{ab} + \Gamma_{ac})$, and $\Delta_3 = \Delta_b - \Delta_c$. In Eqs. (3) the contribution of the local field enters two ways. In (3a), its action is trivial and produces an effective frequency shift, but in (3b) it provides a more significant effect, which is the appearance of the nonlinear coupling between the atomic excitations (polarizations) in the probe σ_{ba} and magnetic σ_{cb} transitions.

Figure 2 shows the comparison of the independent solutions of the exact system (1) and the approximate (3) for different regimes of the atom-field interactions at probe field with the switching time of $\tau_{sw} = 2 \times 10^{-10} \text{ s}$ and cw pump field. The atomic and field parameters were chosen as follows: the characteristic size of the optical beam $a_0 = 20 \mu\text{m}$, the atomic density $\rho = 1.01 \times 10^{22} \text{ m}^{-3}$, the relaxation rate $\Gamma_{ab} = \Gamma_{ac} = 10^9 \text{ s}^{-1}$, the probe field intensity $I_p = 0.22 \text{ W}\cdot\text{cm}^{-2}$, the pump intensity $I_c = 146.5 \text{ W}\cdot\text{cm}^{-2}$, and the probe detuning $\Delta_b = -5 \times 10^9 \text{ s}^{-1}$. The corresponding Rabi frequencies can be calculated as $\Omega = \mu_{ac}E_c/\hbar$ and $g\varepsilon = \mu_{ab}E_p/\hbar$ using the field strengths $E_{c(p)} = \sqrt{I_{c(p)}/c\varepsilon_0}$ and be $\Omega = 1.13 \times 10^{10} \text{ s}^{-1}$ and $g\varepsilon = 4.4 \times 10^8 \text{ s}^{-1}$, respectively ($g = 1.3 \times 10^6 \text{ s}^{-1}$ and $N = 27.7 \times 10^8$). These parameters meet the condition $\Gamma_{ab} < \Omega$ for the strong atom-field coupling in the system.

At near-resonance interaction, when $\Delta_c/d_0\Gamma_{ab} \approx 0.1$ at $d_0 = 0.308$ and $\Delta_c = 3 \times 10^7 \text{ s}^{-1}$, the nonlinear coupling between the probe and pump fields is actually absent as it follows from Fig. 2a. This is due to the fact that during the interaction the ground state $|b\rangle$ is densely populated ($\sigma_{bb} \approx 1$) and atoms at levels $|a\rangle$ and $|c\rangle$ are absent. As a result, the polarizations on transitions $|a\rangle \rightarrow |b\rangle$ and $|a\rangle \rightarrow |c\rangle$ are weak. This regime is

typical for the linear EIT effect in a three-level medium [30], or its non-linear analogue [31] at a significant increase of the pump intensity. However, in this case, the solutions to the Eqs. (1) and (3) for the matrix element σ_{ba} can approximate one another with sufficient accuracy as a proof of validity of approximations used in the derivation of (3).

Quite a different dynamics related to the nonlinear interaction of the fields can be expected when we chose the Raman interaction mode $\Delta_c > \Omega > d_0\Gamma_{ab}$. This interaction regime is well-known [9, 10] and well studied, but it did not get a strong “scientific resonance” in terms of its prospects of practical use in modern optical technologies, as it happened with EIT. This regime is characterized by a set of curves for the matrix elements in Fig. 2b, obtained for the same parameters as in Fig. 2a but with a larger detuning $\Delta_c = 3 \times 10^{10} \text{ s}^{-1}$ and condition $\Delta_c/d_0\Gamma_{ac} \approx 100$. In this case the atomic state $|b\rangle$ is effectively depopulated giving the population mostly to the state $|c\rangle$. This presupposes the emergence of a significant polarization in transition $|a\rangle \rightarrow |b\rangle$. It appears obvious if we compare the scale of values σ_{ba} in Figs. 2a and 2b (the same is true for the transition $|a\rangle \rightarrow |c\rangle$).

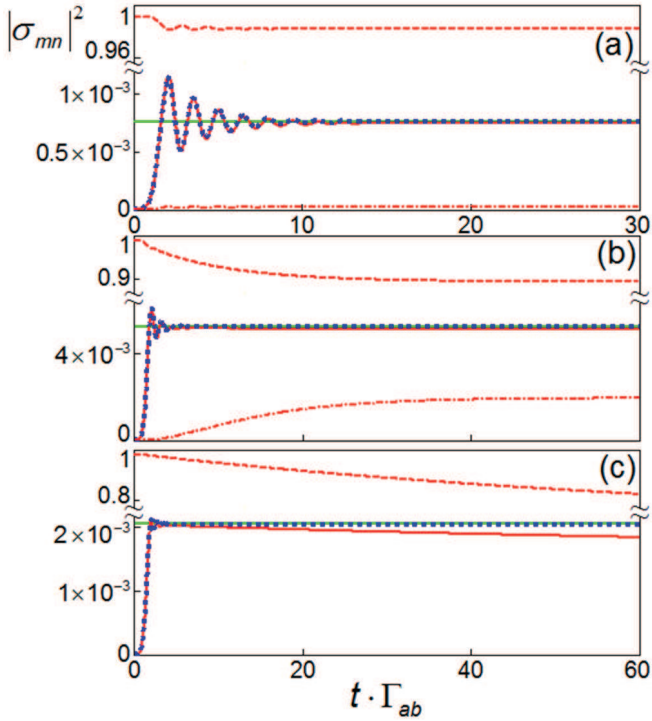


Figure 2. Time dependence of the density matrix elements in units of the excited state lifetime Γ_{ab}^{-1} for (a) the near-resonant and (b) Raman regimes of Λ -type interaction in the limit of strong coupling; (c) for the near-resonant mode in the limit of weak coupling. The thin solid line is for $|\sigma_{bb}|^2$, dashed is for $|\sigma_{cc}|^2$ are solutions of (1), the thick dotted line is for $|\sigma_{ba}|^2$ obtained from Eqs. (3). The thick solid line corresponds to $|\sigma_{ba}|^2$ which is calculated for the approximate steady-state solution (8).

This fact leads to the establishment of a nonlinear energy transfer between the modes of the probe and pump fields. This is the interaction regime we are going to use further in our analysis.

The weak coupling in the atom-field system $\Gamma_{ab} > \Omega$ for both regimes in Figs. 2a and 2b produces a significant discrepancy between the solutions obtained from (1) and (3) as one may see in Fig. 2c at $\Delta_c = 3 \times 10^7 \text{ s}^{-1}$, $\Omega = 1.13 \times 10^8 \text{ s}^{-1}$. In particular, this is due to the violation of the condition $\Omega \gg \sigma_{ca}\chi_{ca}$ and the need to account for the effects of the local field for the transition $|a\rangle \rightarrow |c\rangle$. This fact complicates the problem and requires a direct numerical simulation of the self-consistent problem (2)-(3) [32]. It makes further analysis of opportunities to obtain solitons for this regime very troublesome because of major transformations of the matrix elements.

Now let us find the steady state solution for the density matrix element σ_{ba} of the probe transition in a form that depends only on the material parameters of the media and the characteristics of the optical fields considering various cases of atom-field interaction. In order to do this, we should solve Eqs. (3) in two steps. The first step is to define the polarization of the system at the lower levels σ_{cb} as based on the approximation of constant populations and atomic polarizations in the steady state, i.e., $\dot{\sigma}_{aa} = \dot{\sigma}_{bb} = \dot{\sigma}_{cc} = 0$ and $\dot{\sigma}_{ba} = \dot{\sigma}_{ca} = \dot{\sigma}_{bc} = 0$. At this point we obtain from Eqs. (3) an algebraic equation for the polarization σ_{bc} :

$$\Omega\chi g \varepsilon^* \sigma_{bc}^2 + i \left(\Gamma_1 g^2 |\varepsilon|^2 + \Gamma_2^* A \right) \sigma_{bc} + i g \varepsilon \Omega^* \Gamma_2^* = 0, \quad (4)$$

the roots of which are the following:

$$\sigma_{bc} = \frac{-i \left(\Gamma_1 g^2 |\varepsilon|^2 + \Gamma_2^* A \right) \pm \sqrt{D}}{2\Omega\chi g \varepsilon^*}, \quad (5)$$

where $D = - \left(\Gamma_1 g^2 |\varepsilon|^2 + \Gamma_2^* A \right)^2 - 4i\chi g^2 |\Omega|^2 \Gamma_2^* |\varepsilon|^2$, $A = |\Omega|^2 - i\Delta_3 (\Gamma_1 + i\chi)$, $\chi \equiv \chi_{ba}$.

Solutions (5) determine, in fact, the two branches of spin excitations that occur at the transition between levels $|b\rangle$ and $|c\rangle$ (see Fig. 1). The solution that contains the minus sign in (5) leads to a problem with the saturating nonlinearity $\sigma_{bc} \approx 1/\varepsilon$ and is not considered in this paper. Expansion of the other solution, that is positive, in series of the pump field ε gives the following relationship:

$$\begin{aligned} \sigma_{bc} \approx & -\frac{g\Omega^*}{A}\varepsilon + \frac{g^3\Omega^*}{\Gamma_2^* A^2} \left(\Gamma_1 + i \frac{|\Omega|^2 \chi}{A} \right) |\varepsilon|^2 \varepsilon \\ & - \frac{g^5\Omega^*}{(\Gamma_2^*)^2 A^3} \left(\Gamma_1^2 + \frac{3i|\Omega|^2 \chi \Gamma_1}{A} - \frac{2\chi^2 |\Omega|^4}{A^2} \right) |\varepsilon|^4 \varepsilon. \end{aligned} \quad (6)$$

Our second step is to use the equations for both $\dot{\sigma}_{ca}$ and $\dot{\sigma}_{bc}$ in (3) to write the atomic polarization from the probe transition:

$$\sigma_{ba} = \frac{\left(\Delta_3 + i\frac{g^2|\varepsilon|^2}{\Gamma_2^*}\right)\sigma_{bc} + i\frac{g\varepsilon\chi}{\Omega\Gamma_2^*}|\sigma_{bc}|^2\left(\Delta_3 - i\frac{g^2|\varepsilon|^2}{\Gamma_2}\right)}{\Omega^* - \frac{g^2|\varepsilon|^2\chi^2}{\Omega|\Gamma_2|^2}|\sigma_{bc}|^2} \quad (7)$$

Now we substitute expansion (6) into Eq. (7) and perform

the secondary expansion to get an approximate solution

$$\begin{aligned} \sigma_{ba} \approx & \frac{g\Delta_3}{A}\varepsilon - i\frac{g^3}{\Gamma_2^*A}\left(1 + i\Delta_3\left(\frac{\Gamma_1}{A} + i\frac{\chi}{A^*} + i\frac{\chi|\Omega|^2}{A^2}\right)\right)|\varepsilon|^2\varepsilon \\ & + g^5\left(\frac{1}{(A\Gamma_2^*)^2}\left[i\left(1 - \frac{\chi\Delta_3}{A^*}\right)\left(\Gamma_1 + i\frac{\chi|\Omega|^2}{A}\right) - \frac{\Delta_3}{A}\left(\Gamma_1^2 - 2\frac{\chi^2|\Omega|^4}{A^2} + 3i\frac{\chi\Gamma_1|\Omega|^2}{A}\right)\right]\right. \\ & \left. - \frac{i\chi}{|A|^2|\Gamma_2|^2}\left(i + \frac{\Delta_3}{A^*}\left\{\Gamma_1^* - i\frac{\chi|\Omega|^2}{A^*}\right\} - i\frac{\chi\Delta_3}{A}\right)\right)|\varepsilon|^4\varepsilon. \end{aligned} \quad (8)$$

The solution (8), shown in Fig. 2 with a thick solid line, is in agreement with the solutions (1) and (3) to a high degree of accuracy. This serves as a proof of the correctness of (8). Let us note that if solving Eqs. (3) in the EIT limit, when it can be assumed that $\sigma_{ac} = 0$, the expression for σ_{bc} contains only the first term on the right-hand side of (6) (see [30]). In its turn, Eq. (7) now becomes

$$\sigma_{ba} = \frac{\Delta_3\sigma_{bc}}{\Omega^*} = \frac{g\Delta_3}{A}\varepsilon \quad (9)$$

and determines the appearance of the phase modulation and the absorption (amplification) of the probe pulse in the atomic medium. We found that the appropriate solution for this linear mode (9) for σ_{ba} with sufficient accuracy coincides with the solutions of (1) and (3) in Fig. 2a. The later proves the validity of the theory and the limiting cases as well.

For further analysis we will focus on the situation shown in Fig. 2b and move on to the study of the spatial dynamics of optical beams in the hollow-core fiber filled with resonant atoms as shown in Fig. 1, and consider the possibility of obtaining a special kind of stable structures known as vortex solitons [3] of the probe field.

III. VARIATIONAL APPROACH AND NUMERICAL SIMULATION FOR VORTEX SOLITONS IN A THREE-LEVEL MEDIUM

In the Raman limit for the Λ -type interaction scheme (Fig. 1) after substituting (8) into the propagation equation (2), the self-consistent problem of spatial dynamics (2)-(3) is reduced to the well-known form of the

Ginzburg-Landau equation (see [3]):

$$\left(\frac{1}{c}\frac{\partial}{\partial t} + \frac{\partial}{\partial z}\right)\varepsilon - i\frac{D}{2}\left(\frac{\partial^2\varepsilon}{\partial x^2} + \frac{\partial^2\varepsilon}{\partial y^2}\right) - i\gamma_2|\varepsilon|^2\varepsilon + i\gamma_4|\varepsilon|^4\varepsilon = -\alpha_I\varepsilon - \alpha_2|\varepsilon|^2\varepsilon - \alpha_4|\varepsilon|^4\varepsilon, \quad (10)$$

with the following corresponding coefficients:

$$\gamma_2 = \text{Im}\left\{-\frac{g^4N}{A\Gamma_2^*c}\left(1 + i\Delta_3\left\{\frac{\Gamma_1}{A} + \frac{i\chi}{A^*} + i\frac{\chi|\Omega|^2}{A^2}\right\}\right)\right\}$$

is the cubic nonlinearity;

$$\begin{aligned} \gamma_4 = \text{Im}\left\{\frac{ig^6N}{c}\left(\frac{1}{(A\Gamma_2^*)^2}\left[i\left(1 - \frac{\chi\Delta_3}{A^*}\right)\left(\Gamma_1 + i\frac{\chi|\Omega|^2}{A}\right) - \frac{\Delta_3}{A}\left(\Gamma_1^2 - 2\frac{\chi^2|\Omega|^4}{A^2} + 3i\frac{\chi\Gamma_1|\Omega|^2}{A}\right)\right]\right.\right. \\ \left.\left. - \frac{i\chi}{|A|^2|\Gamma_2|^2}\left(i + \frac{\Delta_3}{A^*}\left\{\Gamma_1^* - i\frac{\chi|\Omega|^2}{A^*}\right\} - i\frac{\chi\Delta_3}{A}\right)\right)\right\} \end{aligned}$$

is the quintic nonlinearity;

$$\alpha_I = \text{Im}\left\{\frac{g^2N\Delta_3}{Ac}\right\}$$

is the linear loss coefficient;

$$\alpha_2 = \text{Re}\left\{\frac{g^4N}{A\Gamma_2^*c}\left(1 + i\Delta_3\left\{\frac{\Gamma_1}{A} + \frac{i\chi}{A^*} + i\frac{\chi|\Omega|^2}{A^2}\right\}\right)\right\}$$

is the cubic loss;

$$\alpha_4 = \text{Re} \left\{ \frac{ig^6 N}{c} \left(\frac{1}{(A\Gamma_2^*)^2} \left[i \left(1 - \frac{\chi\Delta_3}{A^*} \right) \left(\Gamma_1 + i\frac{\chi|\Omega|^2}{A} \right) - \frac{\Delta_3}{A} \left(\Gamma_1^2 - 2\frac{\chi^2|\Omega|^4}{A^2} + 3i\frac{\chi\Gamma_1|\Omega|^2}{A} \right) \right] - \frac{i\chi}{|A|^2|\Gamma_2|^2} \left(i + \frac{\Delta_3}{A^*} \left\{ \Gamma_1^* - i\frac{\chi|\Omega|^2}{A^*} \right\} - i\frac{\chi\Delta_3}{A} \right) \right) \right\}$$

is the quintic loss.

It is clear that Eq. (10) is the result of a complicated nonlinear interaction between the probe field and the pump field which arises solely due to the presence of significant values of polarizations of the optical transitions in the Λ -configuration [11]. Even though the locally acting field used in this theory does not produce new terms in Eq. (10) it, however, gives certain corrections to the picture of the nonlinear interaction (terms with χ -factor) for the case of an optically dense medium. Let us note that in another limit of the Λ -configuration the near-resonance conditions, i.e. $\Delta_b \ll \Gamma_{ab}$, would simplify Eq. (10) by eliminating its nonlinear terms. The local field in this case would be insignificant as it can only lead to an additional phase modulation in the probe field [33].

In order to start the analysis of (10) we will first transform to the moving coordinate system $T = t - z/c$ and perform the change of variables $u = \varepsilon/\sqrt{|\varepsilon_{in}|^2}$, $\xi = z/L_{df}$, $X = x/a_0$, $Y = y/a_0$. Our second step is to define the following main characteristic lengths: $L_{\gamma_2} = 1/(\gamma_2|\varepsilon_{in}|^2)$ and $L_{\gamma_4} = 1/(\gamma_4|\varepsilon_{in}|^4)$ are the nonlinearities of the third and the fifth orders respectively; $L_{\alpha I} = 1/\alpha_I$ describes the linear losses, $L_{\alpha 2} = 1/(\alpha_2|\varepsilon_{in}|^2)$ and $L_{\alpha 4} = 1/(\alpha_4|\varepsilon_{in}|^4)$ describe the nonlinear losses of the third and fifth orders; $L_{df} = a_0^2/D$ is the diffraction length, where ε_{in} is the reduced amplitude of the beam at the entrance point. After multiplying both sides of (10) by L_{df} we finally get

$$i\frac{\partial U}{\partial \xi} + \frac{1}{2} \left(\frac{\partial^2 U}{\partial X^2} + \frac{\partial^2 U}{\partial Y^2} \right) + |U|^2 U - \nu |U|^4 U = Q, \quad (11)$$

where $Q = i[-\delta U - \phi |U|^2 U - \mu |U|^4 U]$ is the dissipative part, for which we have the following notations $U = uN$ and $N^2 = L_{df}/L_{\gamma_2}$, and the main characteristic parameters: $\delta = L_{df}/L_{\alpha I}$, $\phi = L_{\gamma_2}/L_{\alpha 2}$, $\mu = L_{\gamma_2}^2/(L_{\alpha 4}L_{df})$, $\nu = L_{\gamma_2}^2/(L_{\gamma_4}L_{df})$.

For the formation of a conservative optical soliton the interaction parameters should be selected in such a way that the characteristic nonlinear and diffraction lengths were approximately comparable or multiples of each other [34]. This can be achieved near the region of strong transformations of the nonlinear coefficients by varying the detuning of the pump field as it is shown in Fig. 3. In particular, for the point A with detuning Δ_c^A the diffraction length should be only $L_{df} = 1.61$ mm so

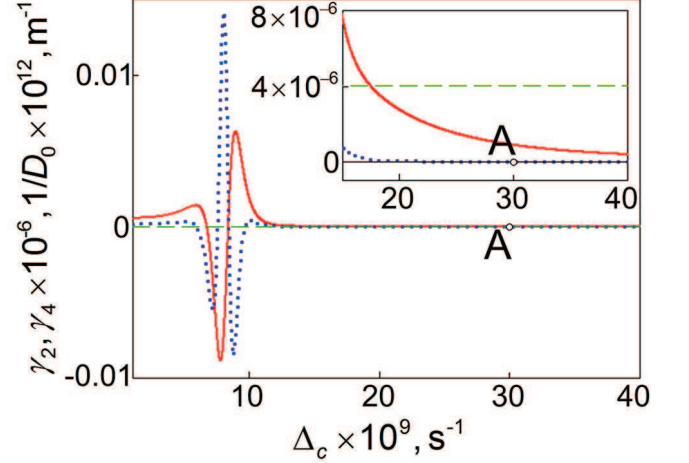


Figure 3. Frequency dependences of the third γ_2 (solid line) and fifth-order γ_4 (dotted line) nonlinearities, and the backward diffraction (dashed line). The inset shows the enlarged image of the region near the point A. The interaction parameters are the same as in Fig. 2(b).

for the positive nonlinearity, i.e. $\gamma_2 > 0$, we may expect focusing and formation of a stable spatial soliton. However, following the concept of dissipative solitons, to maintain the energy of bright solitons it would require interchanging between absorption and gain effects in different areas of the special envelope in cross-section of probe beam. In particular, these conditions can be realized when necessary inequalities $\delta > 0$, $\phi < 0$, $\mu > 0$ are to be met [35]. Figure 4 shows the typical dissipative parameters as functions of the pump field intensity I_c at a fixed detuning Δ_c^A as in Fig. 3 near the gain threshold. Under conditions of differently directed variation of the dissipative coefficients with increasing pump intensity we can select I_c for fixed Δ_c^A (or vice versa) to satisfy the condition of dynamic equilibrium for nonlinear and dissipative processes in the system.

Using the variational approach for the analysis of (11) we may determine the ranges of parameters for which stable spatial solitons can occur. Our particular interest is focused on an important class of dissipative spatial vortex solitons of the kind described in [3]:

$$U = A_0 A \left(\frac{r}{R_0 R} \right)^S \exp \left\{ -\frac{r^2}{2(R_0 R)^2} + i \left(C \frac{r^2}{R_0^2} + S\theta + \Psi \right) \right\}, \quad (12)$$

where $r = \sqrt{X^2 + Y^2}$, θ is the angle in spherical coordinates and A , R , C , and Ψ are the amplitude, the spatial width, the curvature of the wave front and the phase of the soliton, respectively. Parameter S determines the topological charge of the vortex soliton. In the special case of $S = 1$ the normalization coefficients A_0 and R_0

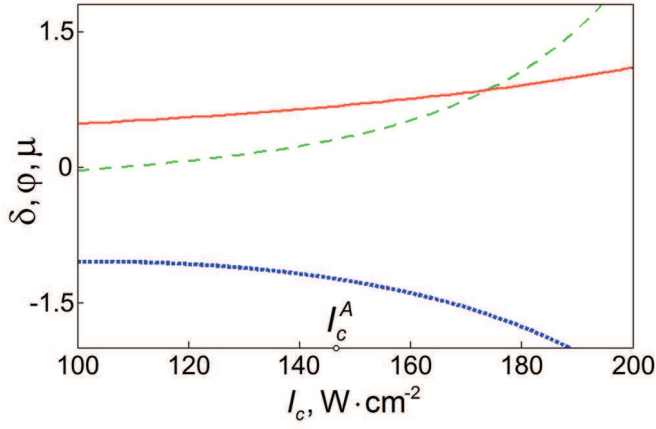


Figure 4. Parameters of the dissipative part of the non-dimensional Ginzburg-Landau equation δ (solid line), ϕ (dotted line), and μ (dashed line) as functions of the pump field intensity. The interaction parameters are the same as for point A in Fig. 3.

can be expressed in terms of the full power normalization

$$P = \int_0^{2\pi} \int_0^\infty |U(r, \theta)|^2 r dr d\theta = (\pi S! A_0^2 R_0^2) A^2 R^2.$$

In the simplest case, when $P = A^2 R^2$, they are related as $A_0 = 1/(R_0 \sqrt{\pi})$ and $R_0 = 1$.

For a self-maintained special crater-shaped vortex solitons (12) the system would require not only a balance of the nonlinear, diffraction and dissipation effects [35] but also some presence of the optical diffusion [36] or a complicated type of modulation of either the refractive index [37] or the absorption coefficient [3] or both. In particular, the static parameter of the linear absorption can be replaced with a space-dependent effective parameter $\delta_{\text{eff}} = \delta - V r^2$. It would describe introduction of an additional saturable absorber into the fiber filled with a cold gas. This is the case we consider further in this paper and assume $V = -0.03$ everywhere below. A detailed analysis of the stability of vortex solitons in the linearization of the master equation written in a form more general than (10) and with the optical diffusion taken into account is given in [38].

Now we use the Euler-Lagrange equation for (11)–(12) and we get the system of equations for the variable parameters:

$$\frac{dA}{d\xi} = -\frac{5\phi A^3}{16\pi} - \frac{8\mu A^5}{81\pi^2} + A(-\delta - C + V R^2), \quad (13a)$$

$$\frac{dR}{d\xi} = \frac{\phi A^2 R}{16\pi} + \frac{2\mu A^4 R}{81\pi^2} + C R + V R^3, \quad (13b)$$

$$\frac{dC}{d\xi} = -C^2 + \frac{1}{8R^4} - \frac{A^2}{16\pi R^2} + \frac{2\nu A^4}{81\pi^2 R^2}, \quad (13c)$$

$$\frac{d\Psi}{d\xi} = \frac{3A^2}{8\pi} - \frac{10\nu A^4}{81\pi^2} - \frac{1}{2R^2}. \quad (13d)$$

For a low frequency modulation ($C^2 \cong 0$), as in [3], we come to the following system of equations, which simplifies the search for the fixed points for (13):

$$C = \frac{A^2 (-81\pi\phi - 32A^2\mu)}{1296\pi^2} - \frac{162\pi^2 V}{A^2 (81\pi - 32A^2\nu)}, \quad (14a)$$

$$R^2 = \frac{162\pi^2}{A^2 (81\pi - 32A^2\nu)}, \quad (14b)$$

$$-\frac{5\phi A^3}{16\pi} - \frac{8\mu A^5}{81\pi^2} + A(-\delta - C + V R^2) = 0. \quad (14c)$$

Equations (14) give 16 steady state roots, among which only two correspond to the physical conditions on the energy and the width of the vortex soliton ($A > 0, R > 0$ and $A, R \in \Re$). Besides, only one of them would have the maximum value of A and negative C and be stable [3].

Figure 5 shows the parametric plane formed by the following parameters: the density of resonant atoms in the system ρ and the intensity of the pump field I_c . The region bounded by the dash-dot line refers to stability of axisymmetric vortex solitons and arise for the selected physical solution of (14) [3]. This area was determined from the analysis of the eigenvalues of the Jacobi matrix for Eqs. (13), i.e., for condition $Re(\lambda_j) < 0$, where $j = 1, 2, 3$ [39], and corresponds to the point of a stable focus.

Direct numerical simulations of Eq. (11) taking into account the initial angular perturbations for R and C [40] in (12) show that the true stability area for axisymmetric vortex soliton I (in Fig. 5) is much smaller. The region of stability obtained using the variational approach appears to have a “fine” structure in the form of separate zones for solitons with modified shapes.

In particular, in the area II in Fig. 5 (parameters as in Eq. (11): $\nu = 0.1653, \delta = 0.6819, \phi = -1.1998, \mu = 0.2432$ at $\rho = 9.85 \times 10^{21} \text{ m}^{-3}$ and $I_c = 146.2 \text{ W}\cdot\text{cm}^{-2}$ for point B) we find a spontaneous transition of an axisymmetric vortex into a single-humped asymmetric stable vortex soliton, presented in image B in Fig. 6. Bifurcations of this type are described in [3]. Region III in Fig. 5 (parameters as in Eq. (11): $\nu = 0.2519, \delta = 0.7158, \phi = -1.2576, \mu = 0.3169$ at $\rho = 9.85 \times 10^{21} \text{ m}^{-3}, I_c = 152 \text{ W}\cdot\text{cm}^{-2}$ for point C) is characterized by a high sensitivity of the system to initial angular perturbations. During the propagation the vortex soliton spontaneously loses its topological charge and transforms into a new vortex-free stable state with $S = 0$ (see image C in Fig. 6).

In area V the account for angular perturbation in Eq. (12) leads to destruction of vortex solitons and emergence of nonstationary localized structures in their place, which, however, do not damp in time and demonstrate some ongoing evolution [41]. At point D in Fig. 5 the parameters in Eq. (11) take values $\nu = 0.1043, \delta = 0.674, \phi = -1.14, \mu = 0.1551$ at $\rho = 9.6 \times 10^{21} \text{ m}^{-3}$ and $I_c = 143.3 \text{ W}\cdot\text{cm}^{-2}$. Here the axisymmetric vortex soli-

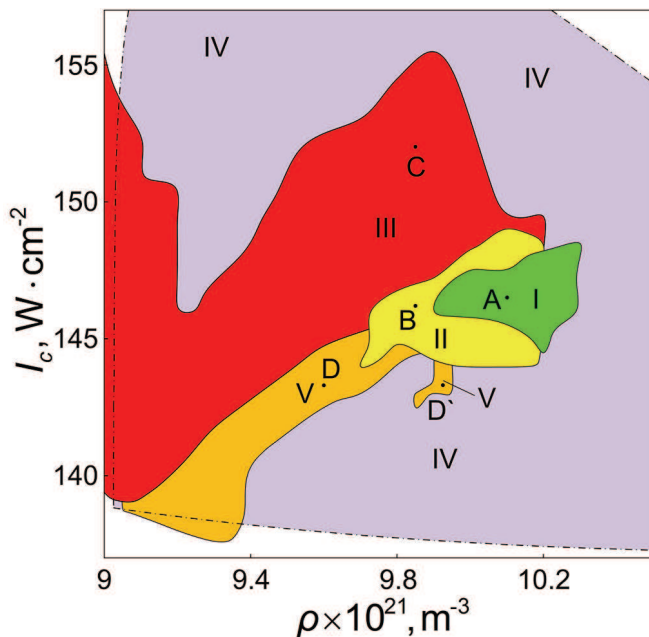


Figure 5. Parametric plane (the intensity of the pump field I_c vs the dopant density ρ). The dash-dot line margins the area of stability for an axisymmetric vortex soliton obtained by the variational approach. The allocated areas are obtained by direct numerical simulations and correspond to: I - axisymmetric vortex solitons, II - single-hump vortex solitons, III - fundamental solitons, V - nonstationary localized structures, IV - unstable structures. The interaction parameters correspond to Fig. 4.

ton transforms in a multi-hump structure rotating during its propagation as in image D in Fig. 6. It is also possible to observe a specific double-hump optical structures [38] as in image D' in Fig. 6. This structure occurs when $\nu = 0.1297$, $\delta = 0.6633$, $\phi = -1.1848$, $\mu = 0.228$ at $\rho = 9.925 \times 10^{21} \text{ m}^{-3}$ and $I_c = 143.3 \text{ W}\cdot\text{cm}^{-2}$. In area IV we notice the loss of stability and complete damping of optical solitons.

Let us note that point A (with the same set of parameters as in Fig. 3) is indeed found in the area of stability, calculated using both the variational approach and direct simulations, which is in agreement with the qualitative analysis of Eq. (11). Thus, formation of vortex solitons in our medium with conditions for point A in Fig. 5 would require the initial spatial width and the curvature of the wave front of the optical soliton in the form of Eq. (12) be $r_R = 19 \text{ }\mu\text{m}$ and $C_R = -3.7 \times 10^6 \text{ m}^{-2}$ respectively. The dimensionless parameters are, therefore, $A = 5.75$, $R = 0.95$, and $C = -0.0015$. The values calculated for Eq. (11) for this regime are $\nu = 0.1899$, $\delta = 0.675$, $\phi = -1.2375$, and $\mu = 0.3075$. The stabilization of optical vortices is achieved within the characteristic length of $L_{ST} = 4 \text{ cm}$ while its rotation period is $T_V = 1.45 \text{ cm}$ (see image A in Fig. 6).

Figure 7 shows the region of stability for vortex solitons in the plane (I_c, V) at $\rho = 1.015 \times 10^{22} \text{ m}^{-3}$. The area

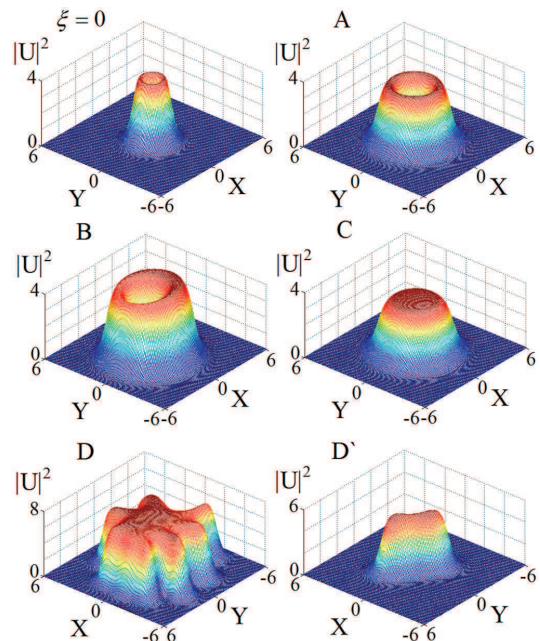


Figure 6. Results of direct numerical simulations of Eq. (11), i.e. spatial shapes in (X, Y) -plane of optical beams at the entrance $\xi = 0$ and after propagation the distance of $\xi = 100000$ in the gas-filled fiber in the presence of azimuthal perturbations. The letter in the upper left corner of each image corresponds to a point in the parameter plane in Fig. 5, the coordinates of which were used to calculate the parameters of the Eq. (11).

of stability obtained by the variational approach extends to both the positive and negative values of parameter V . The direct numerical simulation of Eq. (11) gives a narrower area and demonstrates that stable dissipative vortices can exist only for negative values of V .

The fundamental point in this problem is consideration of the local field effects. Indeed, if $\chi = 0$, the area of stability is not simply transformed, but it completely transcends the parametric plane shown in Fig. 4. In this case, all the solutions obtained for the optical solitons on the parametric planes in Figs. 5, 7 become unstable.

Further analysis and exploration of the other stability areas for the vortex solitons require solution of the full nonlinear system (13) as well as an expanded multi-dimensional numerical experiment within the domain of the system's parameters.

IV. STABILITY STRESS TESTING OF OPTICAL VORTICES UNDER PERTURBATIONS OF SYSTEM'S PARAMETERS

Let us consider the evolution of an optical vortex soliton (12) in terms of noise fluctuations or/and additional modulations of the optical fields and core-filling gas in the fiber. Such perturbations may be associated with variations of the pump field intensity $I_c(X, Y, \xi) =$

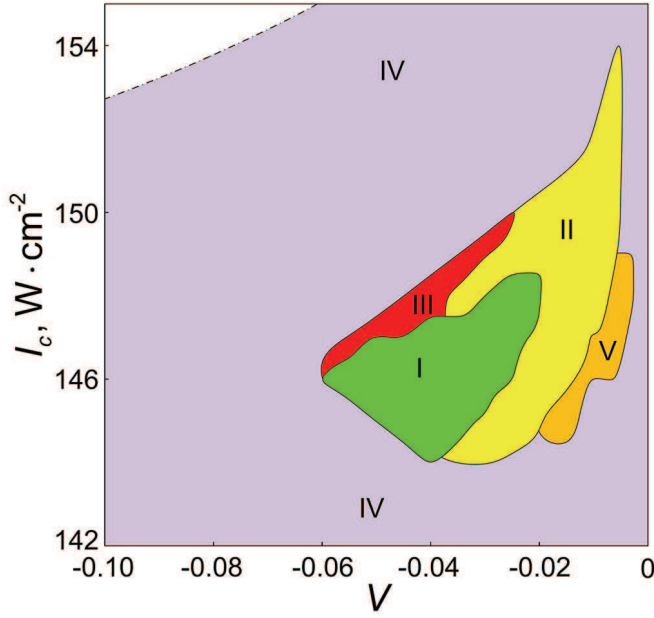


Figure 7. Parametric plane (the intensity of the pump field I_c vs. the optical trapping parameter V). Interaction parameters and numbering of areas are the same as in Fig. 5.

$I_c^{\text{det}} + \zeta_I(X, Y, \xi)$ and the atomic density $\rho(X, Y, \xi) = \rho^{\text{det}} + \zeta_\rho(X, Y, \xi)$, where I_c^{det} and ρ^{det} describe the deterministic part of control parameters. The perturbative parameters $\zeta_I(X, Y, \xi)$ and $\zeta_\rho(X, Y, \xi)$ are presented by three-dimensional matrices of fluctuations or periodic spatial modulation of the corresponding functions. Random perturbations of the intensity $\zeta_I^{\text{rnd}}(X, Y, \xi)$ we describe as the Gaussian white noise. The density fluctuations in a Bose gas below the critical temperature at transformation to the dimensional parameters have a spatial correlation function in the form

$$\langle \zeta_\rho^{\text{rnd}}(r_1) \zeta_\rho^{\text{rnd}}(r_2) \rangle = \rho_0 (\delta(r_1 - r_2) + \nu_n(r_1 - r_2)), \quad (15)$$

where

$$r_i = (z_i, x_i, y_i),$$

$$\nu_n(r_{\text{rnd}}) = \frac{m_a k_B T \rho_b}{\pi \rho_0 \hbar^2 r_{\text{rnd}}} + \frac{3m_0^2 k_B^2 T^2}{4\pi^2 \rho_0 \hbar^4 r_{\text{rnd}}^2}.$$

In our numerical simulations we used the three characteristic spatial scales, i.e., the sampling interval (simulation step) of $\xi_{st} = 0.0011$, the characteristic length of density variation (physical step) of $\xi_{\text{rnd}} = 0.0068$ (equivalent to $r_{\text{rnd}} = 11 \mu\text{m}$) and $\xi_{\text{var}} = 0.07$ for the characteristic distance at which the mean value of the noise becomes zero. The selected physical step is so great that $\nu_n(r_{\text{rnd}})/\rho_0 \approx 0.4\%$, so the second term in the right-hand side of Eq. (15) is neglected and we can model the density fluctuations using the white noise and spatial splines (Fig. 8a,b) for the convenience of calculations at the intermediate points.

The periodic modulation of the pump field intensity $\zeta_I^{\text{reg}}(\xi)$ and the atomic density $\zeta_\rho^{\text{reg}}(\xi)$ with the ampli-

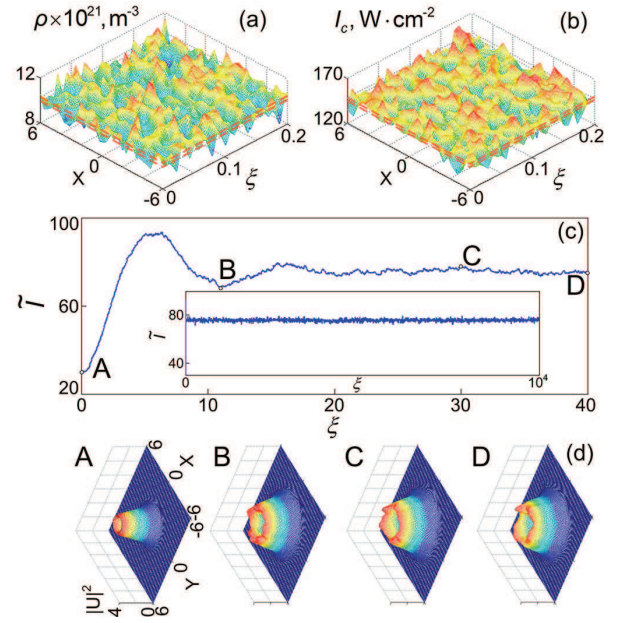


Figure 8. The model of the statistical stability for the axisymmetric vortex solitons with fluctuations of the atomic density ρ (a) and the intensity of the pump field I_c (b). The range of the fluctuating quantities between the dashed lines corresponds to the stability area in Fig. 5. The temporal dynamics of the reduced power \bar{I} of the soliton is shown in image (c), the shapes of the probe optical beam in image (d). The letter at the upper left corner of each image (d) corresponds to the timepoint in image (c).

tudes $\zeta_{I_0}^{\text{reg}}$ and $\zeta_{\rho_0}^{\text{reg}}$ are assumed to be effective only along axis z : $\zeta_I^{\text{reg}}(\xi) = \zeta_{I_0}^{\text{reg}} \sin(2\pi\xi/L_I + \varphi_I)$ and $\zeta_\rho^{\text{reg}}(\xi) = \zeta_{\rho_0}^{\text{reg}} \sin(2\pi\xi/L_\rho + \varphi_\rho)$ with the specified spatial periods L_I , L_ρ and random initial phases $\varphi_{I(\rho)}$. The pulsations of the pump intensity can have two sources: the artificial modulation at the output of the pump laser or the intensity oscillations occurring in the pump depletion and gain saturation [42]. The periodic modulation of the density can be caused by an external mechanical action entailing excitation of acoustic waves in the system.

The specificity of our problem lies in the possibility of studying the generalized picture of the development of perturbations of each GLE parameter and their influence on the dynamics of the soliton via the perturbations of the control parameters for media and the fields. Quantitatively, this may be reflected by the values of the noise strength $D_n = z_{\text{var}}(\sigma_n)^2$ for the GLE coefficients $n = (\gamma_2, \gamma_4, \alpha_I, \alpha_2, \alpha_4)$ with their mean-square deviations σ_n , calculated on the presence of random perturbations for control parameters with the relative deviations $\varepsilon_I = \sigma_I/I_c^{\text{det}}$ and $\varepsilon_\rho = \sigma_\rho/\rho^{\text{det}}$. Here σ_I and σ_ρ are the mean-square deviations for I_c and ρ , respectively; $z_{\text{var}} = \xi_{\text{var}} L_{df}$. The possibility in our numerical simulation of summarized accounting of noise + periodic modulation of the system parameters completes the full-scale stress testing picture for special optical structures which propagate in the hollow-core fiber.

To study the effect of perturbations on the vortex dynamics we performed a series of numerical experiments for different values of σ_I and σ_ρ and the control parameters I_c^{det} and ρ^{det} . As an indirect criterium of stability we assume the statistical stability of the reduced power

$$\tilde{I} = \int_0^{2\pi} \int_0^\infty |U(r, \theta)|^2 r dr d\theta$$

shown in Figs. 8c-10c under perturbations $\zeta_I(X, Y, \xi)$ and $\zeta_\rho(X, Y, \xi)$. If stabilization of \tilde{I} is observed, then we restore and analyze numerically the shape of the soliton in the traced point on axis ξ .

The longitudinal perturbations give rise to the inert properties of the soliton, i.e., the presence of noise, in which the phase trajectories $\rho(X, Y, \xi)$, $I_c(X, Y, \xi)$ never leave the stability region I in Fig. 5, does not cause dramatic consequences. Beyond the stability area the dynamics of a vortex is determined by the retardation effects in slow transformations its shape compared to the rapid changes in GLE parameters initiated by the noise. Figure 8 shows the case of the critical noise parameters $\varepsilon_I^{\text{cr}} = 5.1\%$ and $\varepsilon_\rho^{\text{cr}} = 7.4\%$ ($I_c^{\text{det}} = 146.5 \text{ W}\cdot\text{cm}^{-2}$ and $\rho^{\text{det}} = 10.1 \times 10^{21} \text{ m}^{-3}$ correspond to point A in Fig. 5) for the vortex soliton which preserves its shape over long distances $z = 16.1 \text{ m}$ at $\xi = 10000$ for values of the noise strength $D_\mu = 3.2 \times 10^{-3}$, $D_\nu = 1.1 \times 10^{-3}$, $D_\delta = 1.66 \times 10^{-4}$, $D_\phi = 1.1 \times 10^{-3}$. The increase in parameters $\varepsilon_I^{\text{cr}}$ and $\varepsilon_\rho^{\text{cr}}$ on 0.1% leads to fast damping of a soliton. The presence of the transverse perturbations in plane xOy leads to the noise-induced distortion of the wave packet profile in Fig. 8d but has almost no effect on its stability.

The noise contribution in parameters of Eq. (11) for a regime with $I_c^{\text{det}} = 146 \text{ W}\cdot\text{cm}^{-2}$ and $\rho^{\text{det}} = 9.77 \times 10^{21} \text{ m}^{-3}$ from the transitional area II in Fig. 5 can initiate reduction of topology and a jump transition of vortex solitons in a “breathing” mode in the time point $\xi \cong 1000$ in Fig. 9c. This regime is characterized by constant interconversion between the fundamental soliton and oscillating polygonal structure as on images C, D in Fig. 9d. The observed evolution is the result of migration the optical structure performs between areas III and V in Fig. 5 for values of noise strength $D_\mu = 1.8 \times 10^{-3}$, $D_\nu = 7.23 \times 10^{-4}$, $D_\delta = 1.2 \times 10^{-4}$, $D_\phi = 7.4 \times 10^{-4}$ which correspond to the relative deviations $\varepsilon_I = 1.92\%$ and $\varepsilon_\rho = 2.87\%$ at $\xi_{\text{rnd}} = 0.05$. In the process of transition of a soliton to the vortex-free mode one may observe formation of crescent-shaped optical structure as shown on image B in Fig. 9d. In further rising of ε_I and ε_ρ there comes a transition into an unstable mode and decay, which is associated with a disproportionate increase in the noise strength for various GLE coefficients. In this model for Λ -scheme of interaction the fifth-order nonlinear absorption coefficient μ has a more rapid increase in the noise strength and brings the soliton to zone IV in Fig. 5 and destroys it there.

The destructive effect are also caused by a weak periodic modulation of control parameters in the presence

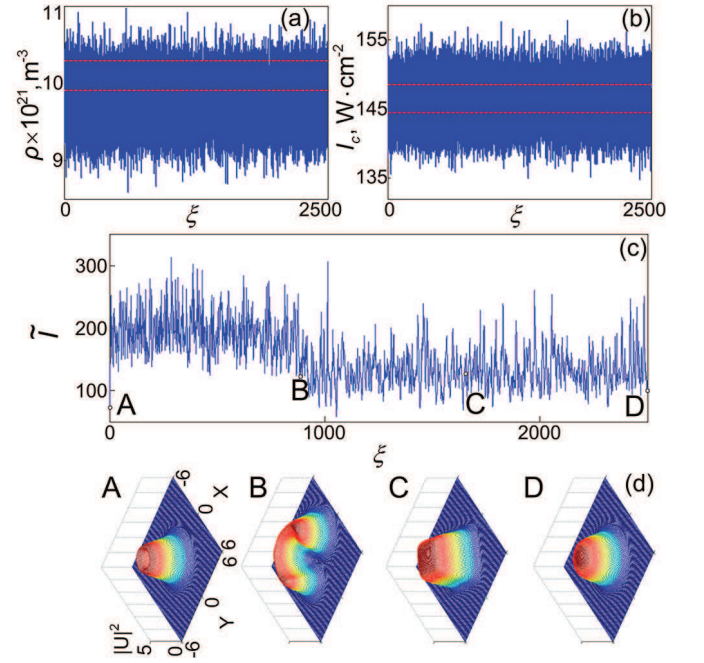


Figure 9. The model of the “breathing” state as a result of migration of the soliton solutions between regions III and V in Fig. 5 in presence of fluctuations (a) the atomic density ρ and (b) the pump intensity I_c . Image (c) shows the temporal dynamics of \tilde{I} ; the probe beam shapes corresponding to different timepoints from (c) are presented in (d).

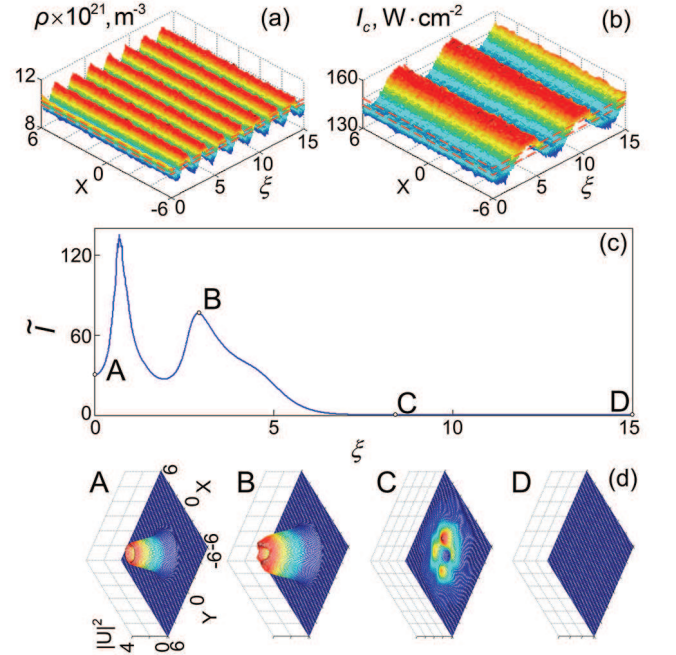


Figure 10. Model of the loss of stability as result periodic modulation of control parameters (a), (b) in the presence of a low-intensity noise. Image (c) shows the temporal dynamics of \tilde{I} ; the probe beam shapes corresponding to different timepoints from (c) are presented in (d).

of a low intensity noise in Fig. 10a,b, which collectively lead to fast violations of dynamic equilibrium in the system and damping of the soliton at scales of the order of $\xi = 8$ in Fig. 10c,d. The simulation parameters correspond to $\zeta_{I_0}^{\text{reg}} = 7.5 \text{ W}\cdot\text{cm}^{-2}$, $\varphi_I = -2.51$ and $\zeta_{\rho_0}^{\text{reg}} = 0.75 \times 10^{21} \text{ m}^{-3}$, $\varphi_\rho = 2.76$, $L_I = 6$, $L_\rho = 2$ at average values of I_c^{det} and ρ^{det} as for point A in Fig. 5. The scale of density fluctuations in Fig. 10a is 3.2 mm that given the expression for the speed of sound in a Bose gas $c_{sn} = (\hbar/m_0)\sqrt{4\pi a_a \rho}$ [43] corresponds to $c_{sn} = 3.2 \text{ mm/s}$ for the sound wave with the frequency 1 Hz. Here m_0 is the mass of a single atom and a_a is the scattering amplitude. In the process of damping of the vortex soliton the system shows the rapid development of angular perturbations leading to the emergence of two or multi-hump unstable localized structures as for images B, C in Fig. 10d. This behavior is associated with a large spatial scale of the simulated periodic perturbations which keep the vortex in unstable area for a long time.

The well-known estimates for the modern laser systems that are compatible with the telecommunication channels determine the maximum allowable noise level of the output intensity to be not higher than 1%. This estimation by a large margin falls within the considered theory of stability of vortex solitons (compare with $\varepsilon_I^{\text{cr}}$ in Fig. 8). Particle number fluctuations of a Bose gas in the range of $T < T_{\text{cr}}$ have the temperature dependence [44]

$$\sigma_N^2 = \frac{\pi^2}{6\zeta(3)} N \left(\frac{T}{T_{\text{cr}}} \right)^3.$$

This equation provides a simple expression for estimating the maximum-allowable density fluctuation in BEC $\varepsilon_\rho^{\text{max}} = \pi (6\zeta(3)N)^{-1/2} \cong 1.17N^{-1/2}$ under condition that $T = T_{\text{cr}}$. For $N = 3 \times 10^4$ and $\omega_0 = 50 \text{ kHz}$ the critical temperature for gas of ^{87}Rb in the fiber is $72 \mu\text{K}$. The maximum-allowable relative density fluctuations in such a system corresponds to $\varepsilon_\rho^{\text{max}} = 0.68\%$, which is 10 times as low as the critical atomic noise calculated for vortex soliton in Fig. 8. This fact makes it evident to observe the vortex soliton regime at a temperature below the critical temperature for BEC.

In numerical calculations for Figs. 8-10 we also consider the fluctuations of diffraction parameter emerging in the cross-section with the spatial scale within the range of the field's wavelength. This requirement arises from the fact that the present fluctuations of the gas density effectively modulate the refractive index of the medium. They also create a random phase delay, which with the accounting for the finite width of the emission line produce the wavelength noise parameter. However, the simulation shows a statistically stable picture with the presence of local perturbations of soliton shapes even at 2% deviations of λ . This is similar to the initial angular perturbations of the vortex shapes which are smoothed after elimination of the noise.

V. CONCLUSION

In this paper we have studied the influence of optical and temperature-dependent atomic fluctuations on the formation and propagation of optical vortex solitons in dense media realized as hollow-core optical fibers filled with a cold atomic gas in presence of optical pumping. This investigation may give some basic provisions that could be useful for development of optical communication channels using vortex solitons in hollow-core fibers filled with a cold atomic gas. With the given parameters of the fiber and the proper intensity of the probe field one can simultaneously tune the intensity and frequency of the cw pump field to provide the conditions for the soliton propagation regime of vortex structures in the optical system. Because of the nonlinear contribution from the local field effects to development of the competitive optical processes in a dense atomic medium it is necessary to account for the NDD corrections in calculating the values of the control parameters for which we expect appearance of the solitons. For the parameters used in the direct numerical simulations the maximum fluctuations of the pump intensity and the probe wavelength for which the soliton regime is still valid impose minor restrictions on the stability of the pump laser power and the probe laser frequency. The estimates for the atomic fluctuations gives an opportunity to observe the optical vortex solitons in the core-filling gas of the fiber for temperatures smaller than the critical temperature for BEC. The large-scale perturbations in the development of acoustic waves and the modulations of the pump field in the fiber can quickly destroy the soliton propagation regime even if they are of small amplitude.

In practice, for long-term maintenance of the BEC state in the information channel it is possible to use fine fibers filled with a cold atoms [45]. Longer lifetimes of a coherent state in such a system are due to the geometry of the fiber and, in addition, the effect of channeling of atoms at creating the surface light wave along its core, causing the atoms to lose their energy effectively. The estimates given in [45] show that for the density 10^{15} cm^{-3} the temperature inside the fiber drops down to $1.5 \times 10^{-5} \text{ K}$.

However, such an elongated BEC must be assumed as a 1D gas so it is necessary to use some different relations for the fluctuations [46] at which observation of the vortex solitons is possible. Except it, the use of thin hollow-core fibers for optical communication due to the need to create localized optical structures at nanoscale, but in solving such a problem transition to the Maxwell equations for continuous media is impossible, and the effects of the near-field will play a crucial role.

VI. ACKNOWLEDGMENTS

This work was supported by Russian Foundation for Basic Research Grant No. 12-02-31573 mol_a and the

Ministry of Education and Science of the Russian Federation under the program “Scientific and scientific-

pedagogical potential of Russia for innovation” (Project No. 14.132.21.1397).

-
- [1] Y. S. Kivshar and G. Agrawal, *Optical Solitons: From Fibers to Photonic Crystals* (Academic Press, 2003).
- [2] N. N. Rosanov, *Dissipative optical solitons: from Micro- to Nano- and Attosolitons* (FIZMATLIT, 2011).
- [3] V. Skarka, N. B. Aleksić, H. Leblond, B. A. Malomed, and D. Mihalache, *Phys. Rev. Lett.* **105**, 213901 (2010).
- [4] R. Pugatch, M. Shuker, O. Firstenberg, A. Ron, and N. Davidson, *Phys. Rev. Lett.* **98**, 203601 (2007).
- [5] A. Smith and D. Armstrong, *Opt. Express* **11**, 868 (2003).
- [6] K. Bezuhanov, A. Dreischuh, G. G. Paulus, M. G. Schätzel, and H. Walther, *Opt. Lett.* **29**, 1942 (2004).
- [7] P. Genevet, S. Barland, M. Giudici, and J. R. Tredicce, *Phys. Rev. Lett.* **104**, 223902 (2010).
- [8] A. Prokhorov, M. Gubin, A. Leksin, M. Gladush, A. Alodjants, and S. Arakelian, *Journal of Experimental and Theoretical Physics* **115**, 1 (2012).
- [9] A. V. Gorbach, D. V. Skryabin, and C. N. Harvey, *Phys. Rev. A* **77**, 063810 (2008).
- [10] B. J. Herman, J. H. Eberly, and M. G. Raymer, *Phys. Rev. A* **39**, 3447 (1989).
- [11] A. V. Gorshkov, A. André, M. D. Lukin, and A. S. Sørensen, *Phys. Rev. A* **76**, 033805 (2007).
- [12] M. Bajcsy, S. Hofferberth, T. Peyronel, V. Balic, Q. Liang, A. S. Zibrov, V. Vuletic, and M. D. Lukin, *Phys. Rev. A* **83**, 063830 (2011).
- [13] A. B. Fedotov, S. O. Konorov, V. P. Mitrokhin, E. E. Serebryannikov, and A. M. Zheltikov, *Phys. Rev. A* **70**, 045802 (2004).
- [14] E. E. Serebryannikov, A. M. Zheltikov, S. Köhler, N. Ishii, C. Y. Teisset, T. Fuji, F. Krausz, and A. Baltuška, *Phys. Rev. E* **73**, 066617 (2006).
- [15] R.-J. Essiambre, G. J. Foschini, G. Kramer, and P. J. Winzer, *Phys. Rev. Lett.* **101**, 163901 (2008).
- [16] F. A. Hopf, C. M. Bowden, and W. H. Louisell, *Phys. Rev. A* **29**, 2591 (1984).
- [17] D. Kuznetsov, V. Roerich, and M. Gladush, *Journal of Experimental and Theoretical Physics* **113**, 647 (2011).
- [18] R. A. Vlasov and A. M. Lemeza, *Phys. Rev. A* **84**, 023828 (2011).
- [19] M. E. Crenshaw, *Phys. Rev. A* **78**, 053827 (2008).
- [20] K. Dolgaleva and R. W. Boyd, *Adv. Opt. Photon.* **4**, 1 (2012).
- [21] L. F. Mollenauer, P. V. Mamyshv, and M. J. Neubelt, *Opt. Lett.* **21**, 1724 (1996).
- [22] M. Chertkov, I. Gabitov, P. M. Lushnikov, J. Moeser, and Z. Toroczka, *J. Opt. Soc. Am. B* **19**, 2538 (2002).
- [23] R. Graham and T. Tél, *Phys. Rev. A* **42**, 4661 (1990).
- [24] C. Cartes, O. Descalzi, and H. R. Brand, *Phys. Rev. E* **85**, 015205 (2012).
- [25] A. Einstein, *Annalen der Physik* **322**, 549 (1905).
- [26] M. von Smoluchowski, *Annalen der Physik* **326**, 756 (1906).
- [27] S. Giorgini, L. P. Pitaevskii, and S. Stringari, *Phys. Rev. Lett.* **80**, 5040 (1998).
- [28] V. V. Kocharovskiy, V. V. Kocharovskiy, and M. O. Scully, *Phys. Rev. A* **61**, 053606 (2000).
- [29] V. Bagnato, D. E. Pritchard, and D. Kleppner, *Phys. Rev. A* **35**, 4354 (1987).
- [30] M. Fleischhauer and M. D. Lukin, *Phys. Rev. A* **65**, 022314 (2002).
- [31] I. Vadeiko, A. V. Prokhorov, A. V. Rybin, and S. M. Arakelyan, *Phys. Rev. A* **72**, 013804 (2005).
- [32] G. Demeter, D. Dzsotjan, and G. P. Djotyan, *Phys. Rev. A* **76**, 023827 (2007).
- [33] R. Fleischhaker, T. N. Dey, and J. Evers, *Phys. Rev. A* **82**, 013815 (2010).
- [34] G. Agrawal, *Applications of Nonlinear Fiber Optics (Optics and Photonics)* (Academic Press, 2001).
- [35] N. Akhmediev and A. Ankiewicz, *Dissipative Solitons: From Optics to Biology and Medicine (Lecture Notes in Physics)* (Springer, 2008).
- [36] D. Mihalache, D. Mazilu, F. Lederer, H. Leblond, and B. A. Malomed, *Phys. Rev. A* **76**, 045803 (2007).
- [37] D. Mihalache, D. Mazilu, V. Skarka, B. A. Malomed, H. Leblond, N. B. Aleksić, and F. Lederer, *Phys. Rev. A* **82**, 023813 (2010).
- [38] S. Fedorov, N. Rosanov, A. Shatsev, N. Veretenov, and A. Vladimirov, *Quantum Electronics, IEEE Journal of* **39**, 197 (2003).
- [39] L. Pontryagin, *Obyknovennye differentsialnye uravneniya* (Nauka, 1974).
- [40] V. Skarka, N. B. Aleksić, M. Derbazi, and V. I. Berezhiani, *Phys. Rev. B* **81**, 035202 (2010).
- [41] N. Rozanov, S. Fedorov, and A. Shatsev, *Optics and Spectroscopy* **95**, 843 (2003).
- [42] R. V. Johnson and J. H. Marburger, *Phys. Rev. A* **4**, 1175 (1971).
- [43] L. P. Pitaevskii and E. M. Lifshitz, *Statistical Physics, Part 2: Volume 9 (Course of Theoretical Physics Vol. 9)* (Butterworth-Heinemann, 1980).
- [44] H. D. Politzer, *Phys. Rev. A* **54**, 1050 (1996).
- [45] V. Balykin, D. Laryushin, M. Subbotin, and V. Letokhov, *Journal of Experimental and Theoretical Physics Letters* **63**, 802 (1995).
- [46] D. S. Petrov, G. Shlyapnikov, and J. T. M. Walraven, *Phys. Rev. Lett.* **85**, 3745 (2000).